Journal of Applied Fluid Mechanics, Vol. 14, No. 2, pp. 615-625, 2021.
Available online at www.jafmonline.net, ISSN 1735-3572, EISSN 1735-3645.
DOI: 10.47176/jafm.14.02.31717

Fluid-Structure Interaction Simulation of Excess Flow Valve Movement at Different Operating Pressures and Gas Flow Rates

G. Coskun† and H. Pehlivan

Sakarya University, Engineering Faculty, Mechanical Engineering Department, Turkey

†Corresponding Author Email: gcoskun@sakarya.edu.tr

(Received April 16, 2020; accepted August 14, 2020)

ABSTRACT

Excess Flow Valves (EFV) for gas-stop systems is generally used in natural gas pipelines to prevent possible damages or destruction due to gas leakage. It can be used in a wide operating range of pressure, but the shut-off flow rate could be in various values at different pressures since natural gas can easily be compressed and can reach higher density. In this study, shut-off and nominal gas flow which effect on a spring force attached to an EFV system simulation by using Fluid Solid Interaction (FSI) strategy was studied. Furthermore, User Define Function (UDF) adapted to simulation to obtain the time-dependent deformation of the spring. The simulations were repeated at five different operating pressures (1-5 bar) with changing flow rates to show if EFV can shut-off the system or not. Results were validated against experimental data of the EFV to show the consistency of the FSI strategy. Moreover, detailed behaviour information of the EFV obtained by means.

Keywords: Computational fluid dynamics; Fluid solid Interaction; Excess flow valve; Adaptive mesh refinement; Compressibility effect; Natural gas flow.

NOMENCLATURE

EFV	Excess Flow Valve	CFD	Computational Fluid Dynamics
FSI	Fluid Solid Interaction	AMR	Adaptive Mesh Refinement
UDF	User Define Function	BSG	Base Grid Sizes

1. INTRODUCTION

Rapid shutting-off gas leakage following damages based on destructive operations, operating errors, natural events like earthquakes or settlement defective spreading of pipes lines is very important to prevent the harmful accidents to people and properties. Therefore, the EFV system is used in natural gas pipelines to avoid this kind of accidents.

There are several applications to automatically shut-off the gas flow in the pipelines. These valves are mainly grouped into two categories as Emergency shut-off valves, which generally work with an electric motor using sensors, and Excess flow valves (EFV), which generally consist of mechanical parts (Cimellaro *et al.* (2018), AGA (2018)). Using EFV requires the selection of proper equipment (design, spring, clappers, etc.) depending on the gas flow rate and pressure. It is necessary to make a detailed investigation and simulation by using fluid dynamic and mechanic structural sciences to define optimum and more reliable equipment. However, in literature very few scientific studies can be found about EFV systems for an emergency gas stop.

Recent developments on computer simulation software and hardware technologies provide simulation capacity for complex physical phenomenon with high converging attitude. Computational fluid dynamics (CFD) is a proper discipline that can simulate such flow conditions with time-depended strategy, which can provide detailed information on fluids behave as real-time pressure force, compressibility effect, turbulence, etc. Duan *et al.* (2019) used 2D CFD model simulate conic, disk and compensated valve to evaluate performances of different eddy viscosity models. They used the standard k-ε model, realizable k-ε model, k-ω-sst model, V2F model, EB k-ε model and the Lag EB k-ε models. Various turbulence models provided better predictions for three different valve shapes. Saha *et al.* (2014). studied a dynamic simulation for the shut-off and pressure regulating valve. They could predict spool movement and final

spool position by developing a special function to calculate force field on the spool. They used a 2D axisymmetric domain to solve transient CFD simulation.

Mirshamsi and Rafeeyan (2015) analyzed and simulated pipeline inspection gauge for gas pipelines. Different numerical cases used to estimate the stop time.

Song *et al.* (2014) made a direct-operated safety relief valve simulation using transient CFD model. They could obtain flow and dynamic characteristics of a safety relief valve. Srikanth and Bhasker (2009) did a transient flow analysis for a valve using a moving mesh strategy in CFD. They needed to do both transient airflow simulation by using compressible Navier–Stokes equations. However, they couldn't solve the real 3D geometry because of complexity and difficulties in the generation of geometry, grid and convergence of fluid flow equations. Therefore, they decided to extrude 2D geometry for arbitrary thickness to obtain as if it is 3D volume. Another transient CFD simulation for a mechanical valve and flow behaviour according to valve position studied by Cenfan Liu *et al.* (2015). They used a sliding mesh method to mimic the closing of the mechanical valve in 3D CFD model. With this method, they could predict qualitative agreement with experimental observation. Zhang *et al.* (2018) used a CFD simulation with response surface methodology for investigating the pressure relief valve. They compared the results with the experimental performance tests and obtained good predictions. Wei *et al.* (2018) studied experimentally and numerical simulation for vortex valve in rocket motor Velocity and pressure effect in vortex chamber before and after injection were explained. Another simulation and experiment study for various valve lifts were done by Jia *et al.* (2018). They examined different intake ports combination and determined port coefficients.

Besides only using the motion-defined CFD simulations, CFD results can interact with structural simulation tools which improve the reality of the physical behave of the complete mechanism. This method known as FSI is becoming popular to solve more complex physical phenomenon as like forces, deformations and behaviours dynamic working conditions on rotary machines (Kovacevic *et al.* 2011, Ze *et al.* 2011, Tan *et al.* 2015, Pei *et al.* 2012), wing deformation at compressible flows Almedia (2013). and etc. Tomaszewski *et al.* (2020) researched gas purification in spray scrubber. They estimated dust collection efficiency in scrubber geometry using CFD. Jia *et al.* 2019 analyzed flow in port and cylinder for diesel engine valves. The effect of four different inlet port combinations on the airflow rate was determined.

Some other diesel engine valves simulated done by Moussa *et al.* 2019. They presented the effect of velocity, temperature and pressure.

Furthermore moving body FSI simulations can be found in the literature. Gurubasavaraju *et al.* (2018). used FSI method to simulate MR damper piston motion in the cylinder. They obtained a good agreement of experimental result in terms of force versus displacement of the piston and investigated piston motion that affects the fluid domain. Beune *et al.* (2012). did an FSI analysis to investigate high-pressure safety valves operation characteristics. They used a 2D axisymmetric domain to solve transient CFD simulation. Another FSI simulation study on valve motion was done by Zhao *et al.* (2018). They modelled reciprocating compressor valve motion using a 3D CFD model. They simulated the valve motion and pressure pulsation simultaneously as the transient flow inside the compressor. They obtained good prediction when compared to the experimental data. Furthermore Wang *et al.* (2013). similarly simulated a reciprocating compressor in 2D geometry. FSI strategy is applied not just for one-directional motion also used for investigation of elastic structure vibration effects on the flow. Dol *et al.* (2018) studied wall shear stress in pipeline flow for laminar and transition flow regime (Re=1100-2800). The effect of water cuts and pipeline construction are determined experimentally. Schildhauer and Spille-Kohoff (2014) simulated Turek benchmark and kinetics of a reed valve by using FSI to investigate compressed air flow effects.

FSI is becoming an effective and realistic simulation strategy for model physical events. However, working with dynamic mesh models are quite time-consuming at preparing simulation case, and also they are open for defaults at especially 3D CFD models. Recently, adaptive mesh refinement (AMR) strategy, which is an effective tool to simulate dynamic movements, has developed rapidly and also adapted to CFD codes. In this study, the FSI strategy applied in the CFD application was used to simulate the behaviour of compressible natural gas flow and EFV system at different operating pressures and flow rates. AMR was used to solve transient dynamic movement. Simulations were prepared based on experimental data of each operating conditions. Results were validated by comparing simulation results with experimental data of the same model for all operating conditions. The shut-off system did not cut the gas flow for the applied CFD simulations at each nominal flow values for all operating pressures. On the other hand, the shut-off system cut the gas flow at shut-off flow values for all operating pressures.

2. GEOMETRY OF THE EFV FOR EXCESS FLOW VALVE

Figure 1 shows the 3D CAD model of the EFV which is currently used in pipeline applications. The model of GS32/1 (d32/DN25) system varies between 1 and 5 bar EFV which is manufactured by the Pipelife Gas-Stop™ used for studying CFD simulations. This EFV designed for 32 mm radius pipeline applications, has a special spring inside to provide the EFV to be opened position till gas force to reach the sufficient value. Detail information, nominal and shut-off flow values for different operating pressures also obtained from the product catalogue (Pipelife Product Catalog 2016).

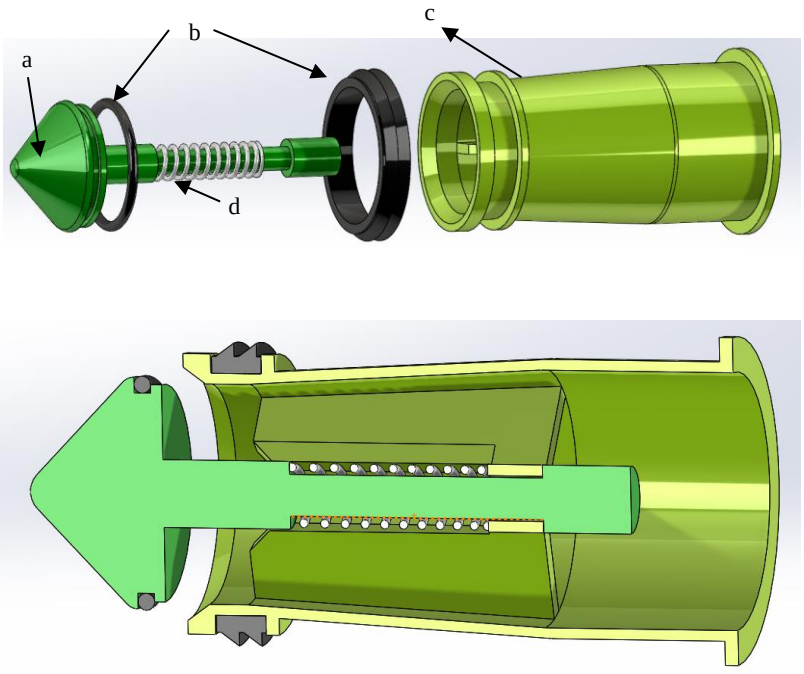

Fig. 1. 3D CAD model and section view of the EFV for gas stop (a: shut-off element, b: seals, c: flow element d: spring).

3. FSI SIMULATION

In this study, CFD simulations were solved by a commercial software package called CONVERGE Converge CFD (2017). The new version of this software gives the option of choosing the spring force effect at FSI mode that was used in this simulation studies.

3.1 Boundary Conditions of the CFD Model

In this simulation study, natural gas was selected as the fluid that needs to be shut-off at emergency cases. If natural gas can be compressed relatively at small pressure changes, density and fluid properties change significantly by affecting the behaviour of the EFV movement. In this study real gas properties were solved by using Redlich-Kwong equation state Redlich and Kwong (1946) by activating compressibility effect at gas flow solver. Simulations were run at 1-5 bar operating conditions that natural gas density could change between 0.7 and 4 kg/m^3 which is directly affecting the force on the shut-off element. The mass fractions of natural gas species used in the simulation study are given in table 1.

Boundary conditions of the simulation case are given as coloured in Fig. 2. Gas inlet and outlet surfaces are equally 10 cm away from the shut-off element seal. Moving bodies that given in the figure are chosen in the software as FSI while the motion of the spring identified by using a UDF.

Table 1 Mass fractions of the natural gas species that used in the CFD simulation

Species	Mass Fraction
CH_4	0.975
C_2H_6	0.008
C_3H_8	0.0045
C_4H_{10}	0.002
IC_5H_{12}	0.0015
N_2	0.003
CO_2	0.006

During the simulation, the spring compresses/expands due to reason i.e. the spring connected to an FSI object. To simulate the compression of the spring, each vertex associated with the spring boundary should be moved as a function of the net compression, vertex location and the displacement of two ends of the spring. For each vertex of the triangulated spring (Fig. 3), there is an associated helix centre. The displacement of the vertex will be the same as the displacement of the helix centre. So, UDF computes the helix centre for the spring, calculate its displacement based on spring compression, and set the vertex displacement equal to the helix centre displacement. For each vertex in the spring, the corresponding centre of helix is computed at UDF. To compute the helix centre H corresponding to a vertex P, a ray is projected normal to the surface, passing through point P. The ray intersects the opposite side of the helix at point Po.

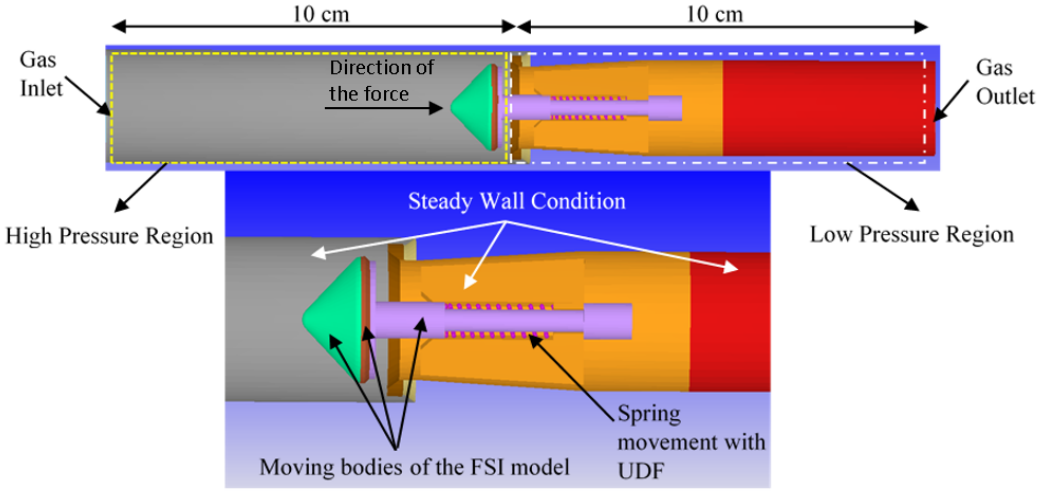

Fig. 2. Boundary conditions of the CFD model.

The average of points P and Po is the helix centre H for point P. Based on the inputs of "end rigid length" and "base rigid length", the length of the spring which compresses is computed. For each vertex that lies within this compressible range, the displacement is set equal to the displacement of its corresponding helix centre.

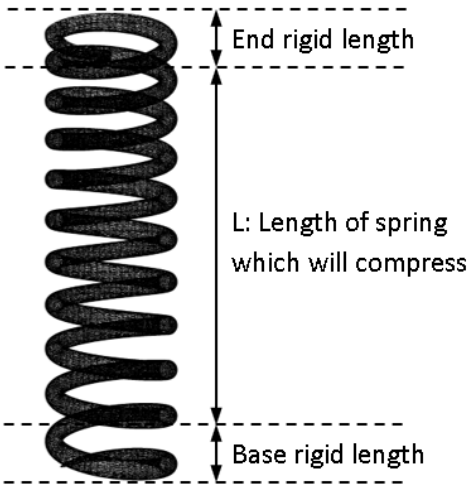

Fig. 3. Spring motion model.

Solution domain was separated into two regions at around flow element seal part as high and low-pressure regions. Gas flow may stop between these two regions when the shut-off element comes near enough to cut the flow with defining an event in the software. In this study, it was defined as "open to gas flow permanently".

The model was solved in full hydrodynamic conditions by using a full transient simulation strategy. The momentum solution for the model was available, but the energy solution was turned off because the temperature has a constant value and it is unnecessary to solve heat transfer for the model. Variable time-step algorithm was used for simulation. Minimum time-step was 1e-11, Maximum time-step was 1. "dt" was changed between 1e-8 and 1e-6 s. Total simulation time for nominal-flow was chosen as 0.01 s while for shut-off flow 0.005 s is enough to complete shut-off movement. RNG k–ε turbulence model Yakhot *et al.* (1992) with the PISO algorithm was used to solve the transient flow of the EFV. Absolute roughness was ignored while roughness constant used as 0.5 for all surfaces. The mass flow rate of the natural gas was defined at the gas inlet by changing for different operating pressure of nominal and shut-off flows. Outlet pressure was used as operating pressure at the gas outlet. The natural gas mass fraction used as 1 for both inlet & outlet boundary conditions and high pressure & low-pressure regions.

3.2 Computational Mesh

CONVERGE includes autonomous adaptive mesh strategy that automatically adjusts the grid as needed at each time-step to appropriately resolve the flow. Figure 4 shows how adaptive mesh strategy effects on the mesh structure for the current case study. When fluid velocity increase, grids become smaller to provide mesh independence at the CFD solution. This technique helps to spend less time in setting the simulation and decreasing total solution-time significantly.

The simulations were run with a grid size of 0.5 mm, 1 mm and different boundary layers for x, y, z coordinates at 3 bar nominal flow case to provide grid-independent solution. Figure 5 (upper images) shows the effect of different grid sizes and boundary layers on the velocity distribution of natural gas around and after the EFV. As the size of the grid decreases, the changes in the velocity profile draw attention. However, the important parameter is flow force and position variation of the shut-off element. Figure 3 (lower images) shows time dependence

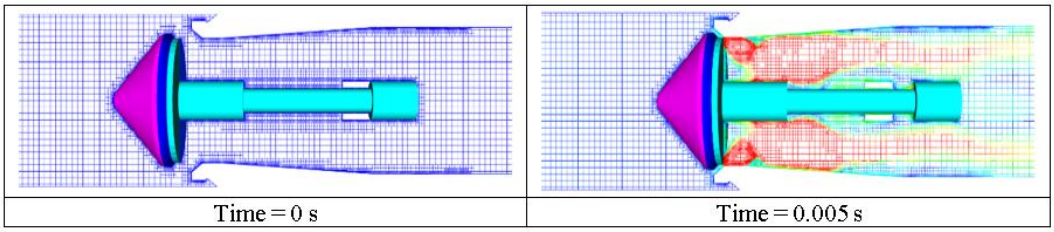

Fig. 4. Example of automatic mesh generation depending on velocity gradient.

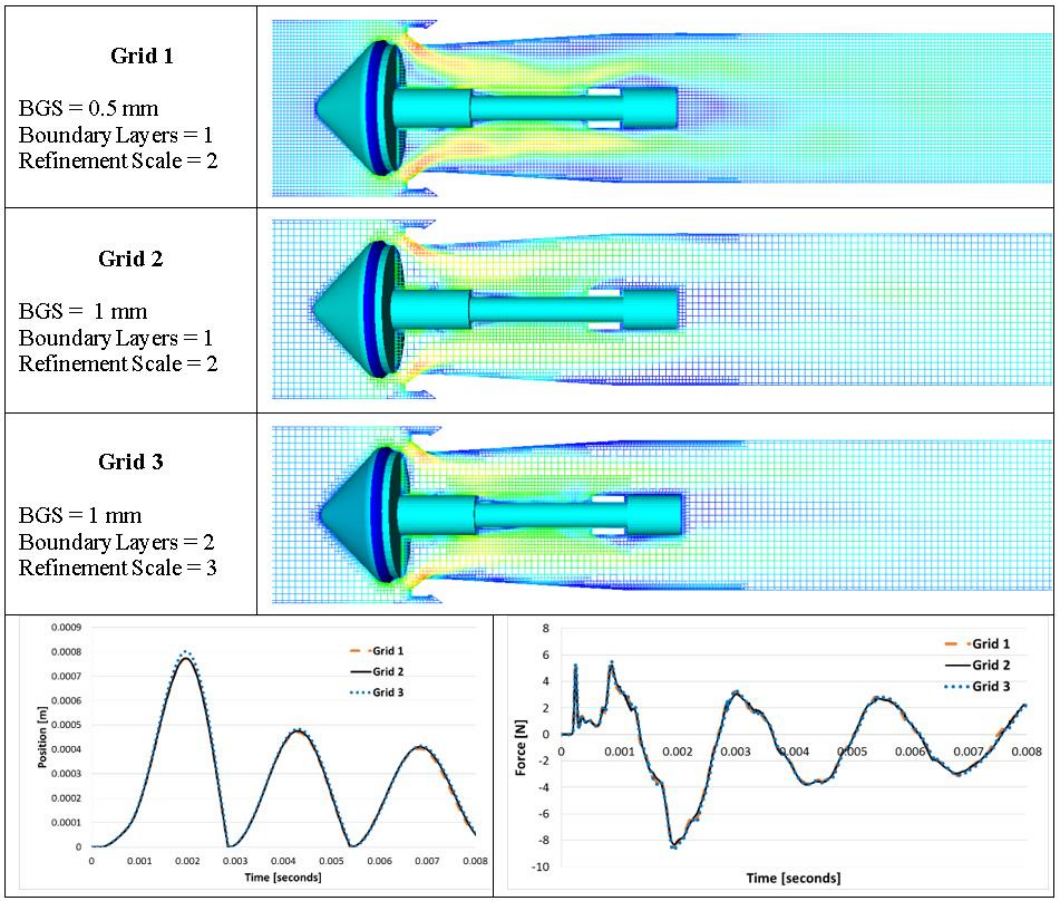

Fig. 5. Upper figures showing different grid size effect on the velocity gradient of natural gas pipe flow. Lower figures showing base grid size effect on the shut-off element position (lower left) and force (lower right).

force on the shut-off element and position changes of shut-off element. Shut-off element position and force values for both two base grid sizes (BGS) and increased layers are matched well so that using smaller grids and increasing boundary layers doesn't affect the shut-off element movement and force. Therefore Grid 2 was chosen for simulations. Approximately 430000 – 445000 total cells were used in transient solution period at Grid 1 for all simulation cases.

4. EXPERIMENTAL PROCEDURE

ASTM standards (Standard Test Method for Performance Testing of Excess Flow Valves-F1802-15) were used in experiments. Besides, the experimental setup was designed and manufactured according to this standard. Air was used as a test liquid for all tests. In Fig. 6, the excess flow valve which is installed in the test apparatus is shown. Inlet pressure is provided to certain places in this device and the flow rate is adjusted. Pressure, temperature and flow values were measured at specific points.

Tests were performed at temperature (19.4 ±5.5°C), pressure (1-5 bar) and flow rate (100-332 m^3/h). The air fluid used in the experiments was corrected by dividing with a f using ρ to determine the nominal and shut-off flow rates of the EFV for the natural gas.

$$f = \sqrt{\frac{0.74}{\rho_{air}}} \tag{1}$$

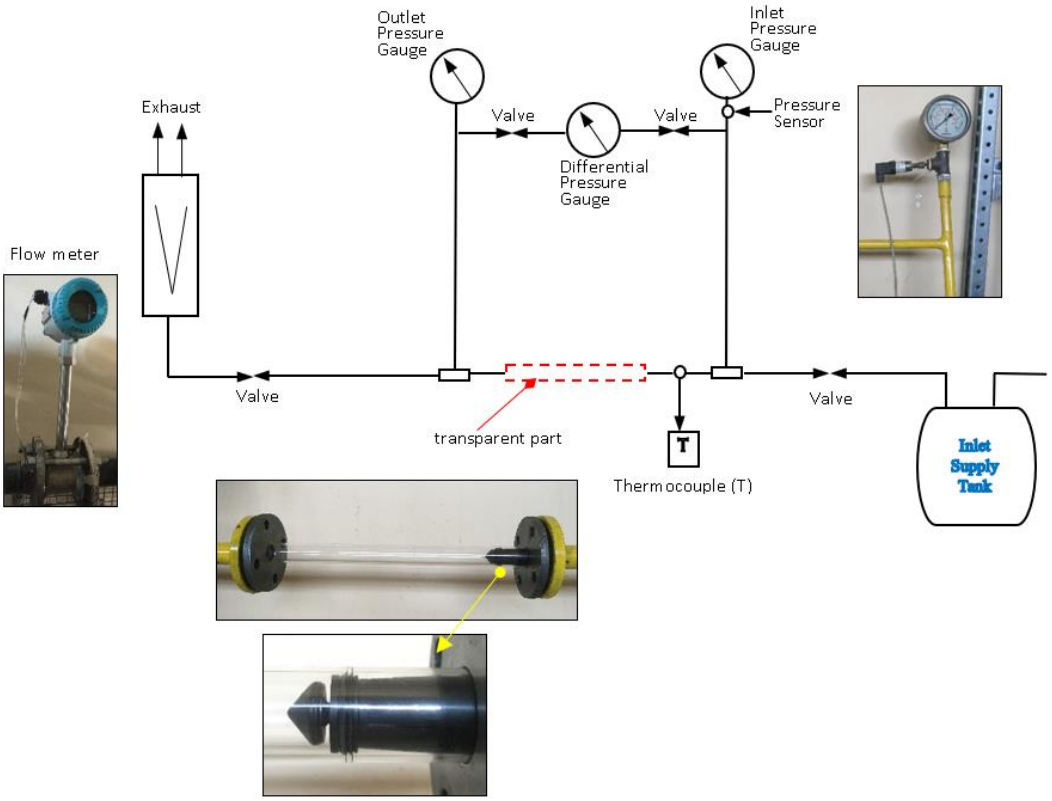

Fig. 6. Experimental setup.

5. SIMULATION RESULTS AND VERIFICATION

Simulations were run by using the experimentaldata for 5 different operating pressures with changing flow rates for nominal and shut-off flows as given in Table 2. According to the obtained results by simulation studies, the shut-off element slightly moves through to the flow element inlet but doesn't cut the flow in nominal flow rates for all operating pressures. On the other hand, the shut-off element completes the movement distance to cut the gas flow in shut-off flow rates.

Table 2 Experimental data of the EFV operating conditions

Operating Pressure [bar]	Nominal flow [m^3/h]	Shut-off flow [m^3/h]
1	100.0	200.0
2	117.5	243.5
3	135.0	274.5
4	151.5	303.0
5	166.0	332.0

Simulation results for the position of the shut-off element depending on time from the beginning of the gas flow are given in Fig. 7. Natural gas flow pressure forces to move the shut-off element slightly. After the shut-off element moves a maximum of 0.001 m at the first turn, it moves back to its original position by the spring resistance. Simulation results at nominal flows show that the shut-off element can stop moving after if its position takes place between 0.2-0.4 mm away from the beginning. At the end of the 0.01 second, the shut-off element moves back and forward four times and the amount of maximum fluctuation decreases each time. It is understanding from figure oscillation frequency decreases with the increasing pressure. Probably because of the high pressure increased gas density causing to decrease in frequency. Because of the long simulation times, only 2 bar nominal flow was continued till 0.05 s to obtain stabilization time. It was seen that oscillation was stabilized after 0.02 second between about 0.15 and 0.3 mm.

If the duration of the simulation were long enough, it is understood from the graphics that the shut-off element motion will be balanced with the spring force after a while. Although the flow rate is 100 m3/h for 1 bar pressure, it was observed that the maximum motion value is higher than the other high-pressure cases. It is seen that this is due to the density change caused by the natural gas being compressible at low pressures, the higher flow velocity at low pressures and therefore flow force coming on to the shut-off element can be a little more.

Figure 8 shows the flow force values at the nominal flows coming on the shut-off element and spring.

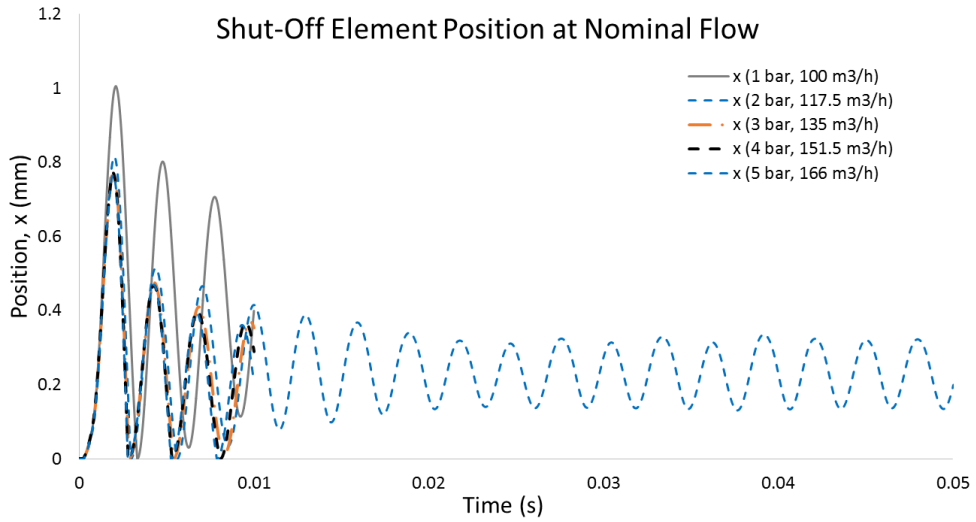

Fig. 7. Simulation results of the time-dependent position of the shut-off element in nominal flow rates.

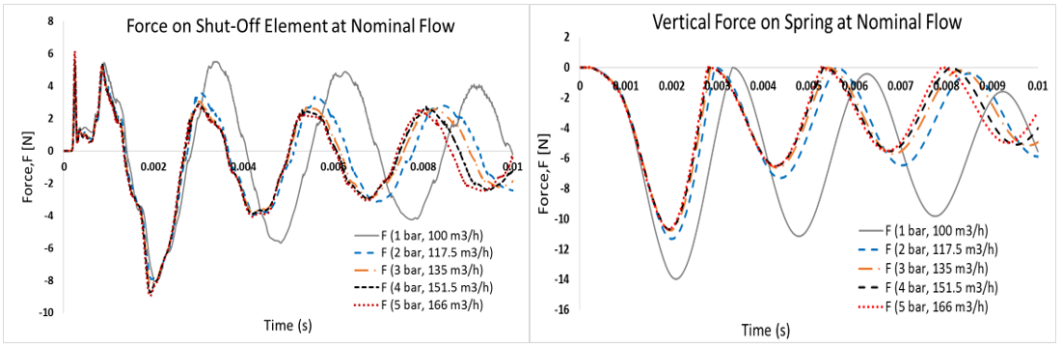

Fig. 8. CFD results of gas flow force on shut-off element and spring for nominal flows at different pressures.

Values for spring represents vertical (z-direction for current case) forces. Shut-off element values represent total force from each direction. Both these forces are not enough to move the shut-off element to cut the gas flow completely. Even though the flow rate at 1 bar pressure, is lower when compared to the other pressures, the flow force coming on to the shut-off element and spring is a little bit higher at 1 bar pressure. It is noticed that the forces, which affect the spring, come closer to each other by the increase of operating pressure. As time passes, the flow and spring forces appear to be in balance.

Simulation results for the position of the shut-off element at shut-off pressures depending on time are given in Fig. 9. Unlike nominal flow data with the increase of operating pressure, the shut-off element is moving faster.

This is probably due to the volumetric flow rate increase is greater than the nominal flow values. Notice that the shut-off element does not close directly. The spring force counteracts the flow force at first, then the shut-off element completes its movement after defeating the spring force completely. Here also shut-off element moves very faster than in the real case. Because simulations directly begin at the shut-off flow rate for all operating pressures. In a real case, flow rate increases while the leakage begins following the damage at pipeline.

Figure 10 shows the force values of the shut-off element and spring during the shut-off flows. As the shut-off element cut the gas flow, the total force of it increases continuously by the reason of continuous flow at the inlet of the model. Simulations show that shut-off element completes its movement around 14 N vertical force. When considering vertical force that is on spring cutoff force, each operating pressure force exceeds 14 N.

Figure 11 shows the natural gas flow velocities at 1 and 5 bar operating pressures for nominal flow rates. The change of the velocity profile around the EFV is seen from Fig. 11. The maximum value of the gas velocity at 1 bar operating pressure is 261.92 m/s while at 5 bar operating pressure is 96.63 m/s. After

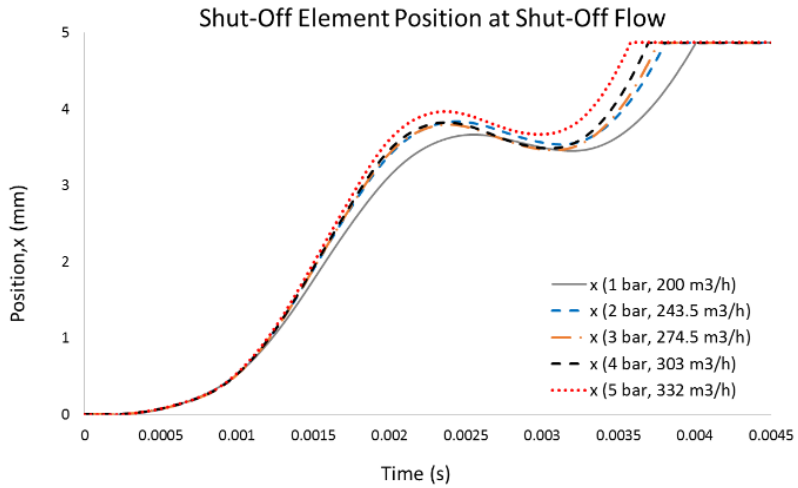

Fig. 9. Simulation results of the time-dependent position of the shut-off element in shut-off flow rates.

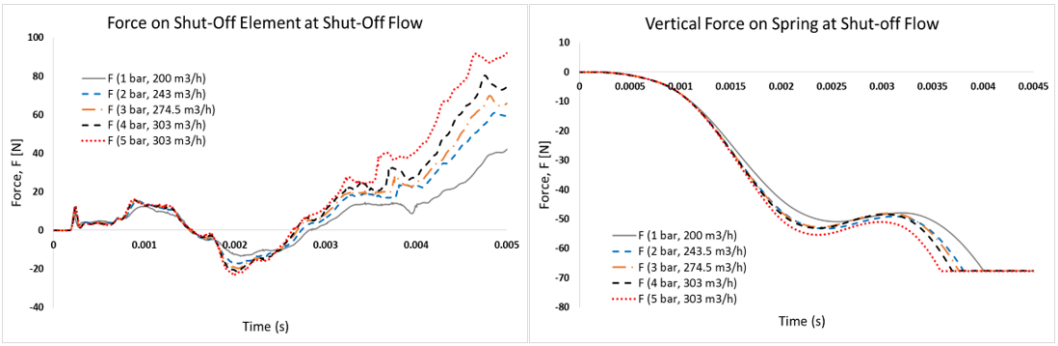

Fig. 10. CFD results of gas flow force on shut-off element and spring for shut-off flow at different pressures.

0.008 seconds, the gas flow at 1 bar pressure is more uniform and stable than the 5 bar flow at the other pipeline.

Figure 12 shows the natural gas flow velocities at 1 and 5 bar operating pressures for shut-off flow rates. It is seen from figures at high operating pressures the shut-off element is seen to move more quickly and effectively due to the high flow rate. This attitude is quite satisfactory. Because the natural gas flow out of the pipe will be much faster after the damage at the high-pressure pipelines, and it is much more important to cut high-pressure gas flow than the low pressure

6. CONCLUSION

Transient CFD simulation procedure of an EFV shut-off element by using FSI and AMR for different operating pressures and flow rates has been considered. A UDF was adapted to the simulation to model dynamic spring movement locating over the shut-off element. Flow rates that experimentally obtained and verified from catalogue data were used as inlet boundary conditions of the simulation. The main aim of the study is to show that the movement of the EFV can be simulate using FSI strategy. Also to obtain detail information about EFV behaviour for both nominal and shut-off flow and different pressures and flow rates

It was understood that decreasing BSG and number of boundary layers didn't affect the position of EFV and force on shut-off element. It can be told that using bigger BSG with a single boundary layer can decrease the total simulation time without effecting results significantly.

With the help of simulation study compressibility effects of natural gas on shut-off, element movement was also investigated. At low pressure, natural gas flows, the vertical force on the spring is a bit higher than others although volumetric flow rate is lower. If the mass flow rate is taken into consideration, this difference will be greater. At low pressures, the shut-off element moves faster in the nominal flow but moves slowly in the shut-off flow. But this situation can be ignored because of the small differences. If there was a pipeline flow system with a very high operating pressure and/or a fluid which has higher compressibility characteristics, this could seriously change the operating conditions.

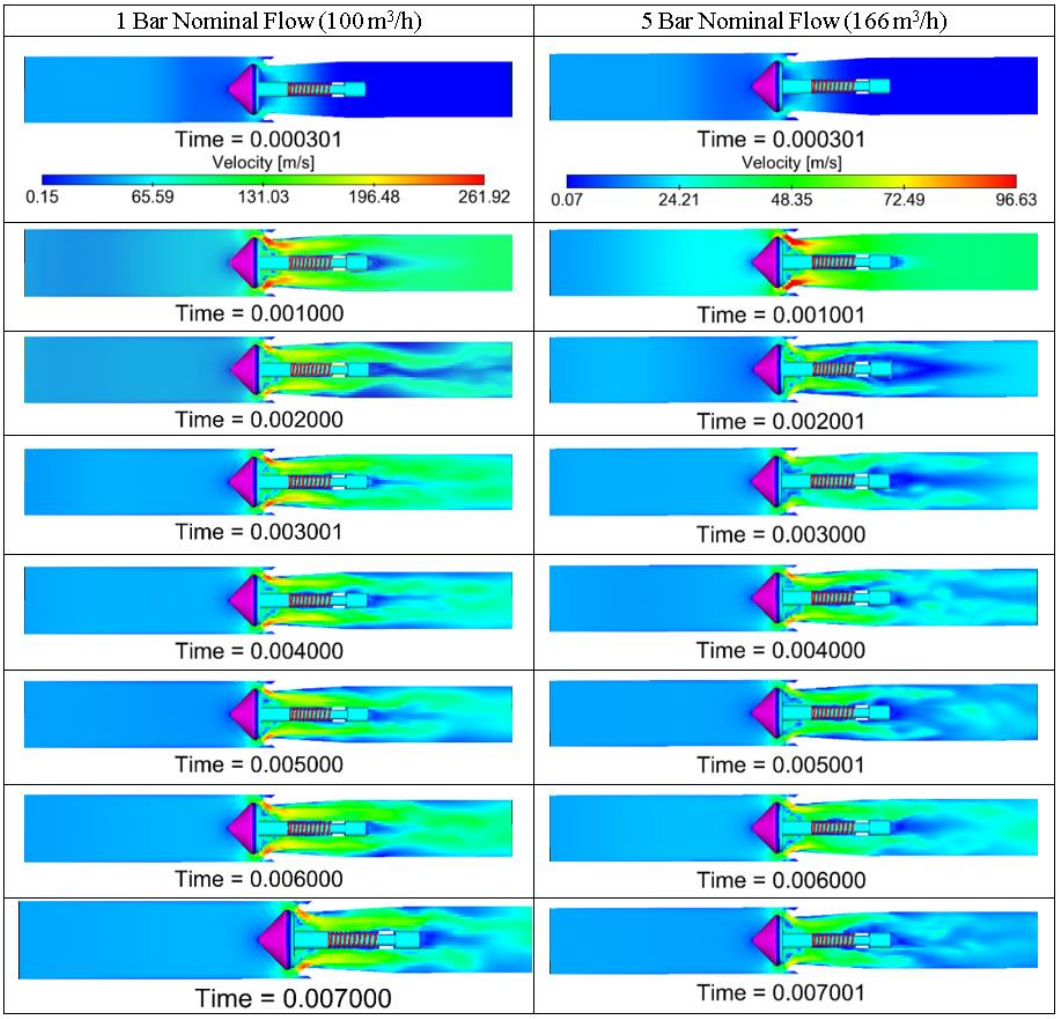

Fig. 11. Visual results of shut-off element position and flow velocity inside the pipeline for 1 and 5 bar operating pressures at nominal flows.

From 2 bar nominal flow oscillation stabilization time was obtained by containing simulation till 0.05 s. It was seen that oscillation was stabilized after 0.02 second and EFV continued to oscillate between about 0.15 and 0.3 mm at the force direction.

FSI simulations can be very useful to improve existing design for different operating conditions or to extend the operating range without performing time-consuming and expensive experimental studies. By using AMR strategy, CPU time could be seriously decreased and complete 3D model could be used to simulate this kind of cases, and by this way optimization studies can be done more effectively for FSI cases.

ACKNOWLEDGEMENT

The authors would like to thank Adapazarı Gas Distribution Corporation (AGDAŞ), Sakarya Techno Park and Sakarya University for supporting this project. This project was financed by AGDAŞ.

REFERENCES

AGA, American Gas Association, (2018) White Paper Automatic Shut-off Valves (ASV) And Remote Control Valves (RCV) On Natural Gas Transmission Pipelines, 2011. http://www.cpuc.ca.gov/uploadedFiles/CPUC_Public_Website/Content/Safety/Natural_Gas_Pipeline/AppendixL.pdf (accessed September 17, 2018).

Beune, A., J. G. M. Kuerten and M. P. C. van Heumen (2012). CFD analysis with fluid–structure interaction of opening high-pressure safety valves. *Computer&Fluids* 64, 108–116.

Cimellaro, G. P., O. Villa and H. U. Kim, Resilience-Based design of Natural Gas Pipelines, in: The 15th World Conference on Earthquake

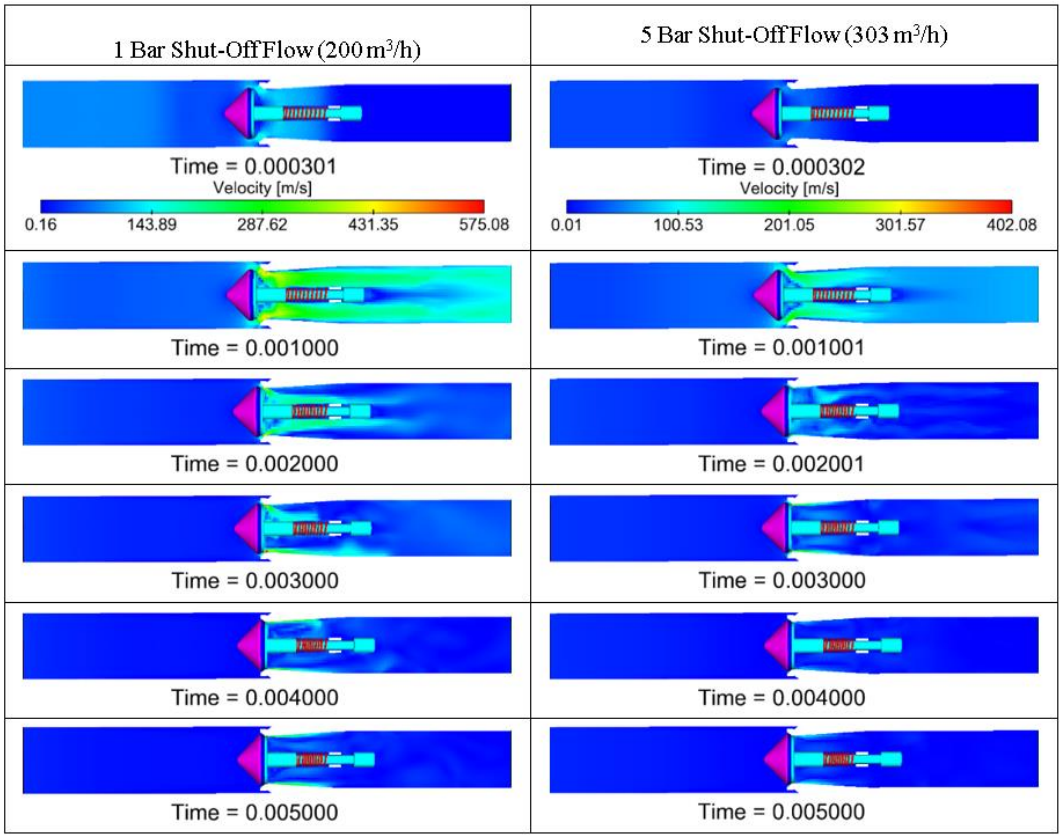

Fig. 12. Visual results of shut-off element position and flow velocity inside the pipeline for 1 and 5 bar operating pressures at shut-off flows.

Engineering, Lisboa, Portugal (2013). https://www.iitk.ac.in/nicee/wcee/article/WCEE2012_5721.pdf (accessed September 17, 2018).

Converge CFD, Version 2.4.14., (2017).

Dol, S. S., S. F. Wong, S. K. Wee and J. S. Lim (2018) Experimental Study on the Effects of Water-in-oil Emulsions to Wall Shear Stress in the Pipeline Flow. *Journal of Applied Fluid Mechanics* 11(5), 1309-1319.

Duan, Y., C. Jackson, M. D. Eaton and M. J. Bluck (2019), An assessment of eddy viscosity models on predicting performance parameters of valves. *Nuclear Engineering and Design* 342, 60–77.

Gurubasavaraju, T. M., H. Kumar and A. Mahalingam (2018). An approach for characterizing twin-tube shear-mode magnetorheological damper through coupled FE and CFD analysis. *Journal of the Brazilian Society of Mechanical Sciences and Engineering* 40, 139.

Jia, D. W., X. W. Deng and J. L. Lei (2018) Steady-State Experiment and Simulation of Intake Ports in a Four-Valve Direct Injection Diesel Engine. *Journal of Applied Fluid Mechanics* 11(1) 217-224.

Jia, D. W., X. W. Deng, Y. Wang and J. L. Lei (2019) Flow field influence analysis of combination intake port and in-cylender for a four-valve diesel engine. *Journal of Applied Fluid Mechanics* 12(3), 871-881.

Kovacevic, A., N. Stosic, E. Mujic, I. K. Smith and D. Guerrato (2011). Extending the role of computational fluid dynamics in screw machines. *Proceedings of the Institution of Mechanical Engineers, Part E: Journal of Process Mechanical Engineering* 225, 83–97.

Liu, C., M. Zhao, W. Wang and J. Li (2015). 3D CFD simulation of a circulating fluidized bed with on-line adjustment of mechanical valve. *Chemical Engineering Science* 137, 646–655.

Mirshamsi, M. and M. Rafeeyan (2015). Dynamic Analysis of Pig through Two and Three Dimensional Gas Pipeline. *Journal of Applied Fluid Mechanics* 8, 43-54.

Moussa, O., A. Ketata, Z. Driss1 and P. Coelho (2019). In-Cylinder Aero-Thermal Simulation of Compression Ignition Engine: Using a Layering Meshing Approach. *Journal of Applied Fluid Mechanics* 12(5), 1651-1665.

Pei, J., F. K. Benra and H. Dohmen (2012). Application of different strategies of partitioned fluid–structure interaction simulation for a single-blade pump impeller. *Proceedings of the*

Institution of Mechanical Engineers, Part E: Journal of Process Mechanical Engineering 226, 297–308.

Pipelife, Product Catalog of Pipelife Gas-Stop, Austria (2016) www.pipelifegasstop.com (accessed April 16, 2020).

Redlich, O. and J. N. S. Kwong (1949). On the Thermodynamics of Solutions. V. An Equation of State. Fugacities of Gaseous Solutions. *Chemical Reviews* 44, 233–244.

Saha, B. K., H. Chattopadhyay, P. B. Mandal and T. Gangopadhyay (2014). Dynamic simulation of a pressure regulating and shut-off valve. *Computer & Fluids* 101, 233–240.

Schildhauer, M. and A. S. Kohoff (2014). Numerical simulation of fluid-structure interaction: Turek benchmark and kinetics of a reed valve. *Progress in Computational Fluid Dynamics: an International Journal* 14, 38.

Song, X., L. Cui, M. Cao, W. Cao, Y. Park and W. M. Dempster (2014). A CFD analysis of the dynamics of a direct-operated safety relief valve mounted on a pressure vessel. *Energy Conversion and Management* 81, 407–419.

Srikanth, C. and C. Bhasker (2009). Flow analysis in valve with moving grids through CFD techniques. *Advances in Engineering Software* 40, 193–201.

Tan, Q., S. Pan, Q. Feng, X. Yu and Z. Wang (2015). Fluid–structure interaction model of dynamic behavior of the discharge valve in a rotary compressor. *Proceedings of the Institution of Mechanical Engineers, Part E: Journal of Process Mechanical Engineering* 229, 280–289.

Tomaszewski, A., T. Przybylinski, P. Kapica and M. Lackowski (2020). Influence of the Spray Scrubber Geometry on the Efficiency of Dust Removal – Theoretical Predictions and CFD Analysis. *Journal of Applied Fluid Mechanics* 13(4), 1055-1066.

Wang, Y., J. Feng, B. Zhang and X. Peng (2013). Modeling the valve dynamics in a reciprocating compressor based on two-dimensional computational fluid dynamic numerical simulation. *Proceedings of the Institution of Mechanical Engineers, Part E: Journal of Process Mechanical Engineering* 227, 295–308.

Wei, X. G., J. Li and G. Q. He (2018). Swirl Characteristics of Vortex Valve Variable-Thrust Solid Rocket Motor. *Journal of Applied Fluid Mechanics* 11, 205-215.

Yakhot, V., S. A. Orszag, S. Thangam and T. B. Gatski, C.G. Speziale, (1992). Development of turbulence models for shear flows by a double expansion technique. *Physics of Fluids A Fluid Dynamics* 4, 1510–1520.

Ze, X. B., Y. W. Sun, W. Wang, J. L. Nie and K. Mao (2011). Analysis of gas—solid coupling flow field in a vertical roller mill under different gas fluxes. *Proceedings of the Institution of Mechanical Engineers, Part E: Journal of Process Mechanical Engineering* 225, 20–28.

Zhang, J., L. Yang, W. Dempster, X. Yu, J. Jia and S. T. Tu (2018). Prediction of blowdown of a pressure relief valve using response surface methodology and CFD techniques. *Applied Thermal Engineering* 133, 713–726.

Zhao, B., X. Jia, S. Sun, J. Wen and X. Peng (2018). FSI model of valve motion and pressure pulsation for investigating thermodynamic process and internal flow inside a reciprocating compressor. *Applied Thermal Engineering* 131, 998–1007.